

ASSESSMENT OF SUB-OPTIMAL SDRE CONTROL SYSTEMS PERFORMANCE BY DEFINING A SET OF RANDOM WEIGHTING MATRICES

Leonardo M. Mazzariol

André Fenili

L.mazzariol@ufabc.edu.br

Andre.fenili@ufabc.edu.br

Engineering, Modeling and Applied Social Sciences Centre (CECS), Federal University of ABC

Av. Dos Estados, 5001, 09210-580, Santo André/São Paulo, Brazil

Abstract. It is well known that the design of a huge class of non-linear control systems depends heavily on the state-space representation of the to-be-controlled system. So, the task of choosing appropriate control parameters for the nonlinear system's stability and performance requirements tends to be time consuming, tedious and relies mostly on the designer's experience. The work presented here evaluates the system performance using sets of random weighting matrices as input for the feedback control technique based on the State-Dependent-Riccati-Equation (SDRE). These randomly generated sets are obtained by using Monte Carlo sampling and UQLab, then evaluated using numerical simulations of two one degree of freedom strongly non-linear systems and a slewing flexible structure. The results showed that these sets serve as an interesting tool to map controllable regions of interest while allowing the designer to visualize the effects of these weights on the system's constraints and the performance requirements of the systems response.

Keywords: stability, SDRE control, nonlinear systems

1 Introduction

Mechanical systems usually require a type of Control Theory in order to assure that their states during service are kept within design envelope, demanding stabilization, tracking, positioning etc. Many of these systems are naturally stable and may not require active control systems. However, the increased complexity due to non-linear phenomena and thus inherent instabilities require the application of active control systems, being the investigation of feedback, Optimal Control, an important area of research [1].

The State-Dependent Riccati Equation (SDRE) strategy offer significant advances when compared to Linear Optimal Control Theory, specially when system states have strong influence in the response. SDRE algorithm is based on a nonunique linear structure having a state-dependent coefficients (SDC) matrices. The control feedback is then calculated by minimising a nonlinear performance index that is based on these SDC and weighting matrices. Since the SDC vary during load, the procedure is calculated every step of integration or when requested [2].

So, due to differences in representation (or parametrisation) for the same system, weighting matrices may produce different results. In addition, there are representations that may be more efficient, stable or sensitive to the weighting matrices. Then, the choice of appropriate weighting matrices may lead to a suboptimal solution, which is the optimal solution for that specific representation, while that global optimal cannot be inferred or maybe never obtained if the ‘best’ SDC is not found [3].

The use of stochastic methods have been widely applied to investigate systems when geometry parameters and material properties are naturally stochastic [4, 5]. Pellissetti and Schuëller [6] integrated commercial finite element code with the sampling of inputs. The deterministic results combined was then used to infer the range of the stochastic response. Hence, evaluating series of simulations with parameters obtained from sampling a distribution may serve as a tool to investigate the sensibility of the system to a particular range and variables. Considering the response of the system according to a SDC representation, varying weighting matrices randomly may result in a desired performance envelope.

Thus, this article investigates the use of random weighting matrices to verify the range of performance of three different dynamic nonlinear models using SDRE control systems. By using these matrices one can obtain a field of possible responses, allowing the designer to better explore the parameters and maybe find a solution closer to the optimal one. In what follows, the three models equations and state-space systems are shown in Sec. 2. A short description of SDRE methods and the importance of Q and R matrices lie in Sec. 3. Section 4 describes the investigation method, by terms of obtaining the random matrices using Monte Carlo method, numerical integration, parameters and initial conditions for all three models. Results are presented in Sec.5, while Sec. 6 encloses the article.

2 Theoretical Models

Three nonlinear models were chosen to explore the method to evaluate systems performance envelope using random weighting matrices. The number of viable (nonunique) SDC representations increases with model complexity, as presented in the following items.

2.1 Model I

The first model is described as simple nonlinear one degree of freedom system, where an inertial term is followed by a nonlinear portion based both on position x and velocity \dot{x} , as

$$m\ddot{x} + \alpha x\dot{x}^2 = F. \quad (1)$$

Equation 1 can be rewritten in terms of state-space variables, $x_1 = x$, $x_2 = \dot{x}$ and its derivatives,

$$\begin{cases} \dot{x}_1 = x_2 \\ \dot{x}_2 = \frac{F}{m} - \frac{\alpha}{m}x_1x_2^2 \end{cases} \quad (2)$$

It is possible to rewrite Eq. (2) in the matricial state-space form

$$\{\dot{x}\} = A(x)\{x\} + B(x)\{u\} \quad (3)$$

being A and B the State-Dependent Coefficients (SDC); x and \dot{x} , the state space vector and its derivative, respectively. That modelling results in two different but equally viable state-space form representation

$$\begin{cases} \dot{x}_1 \\ \dot{x}_2 \end{cases} = \begin{bmatrix} 0 & 1 \\ -\frac{\alpha}{m}x^2 & 0 \end{bmatrix} \begin{cases} x_1 \\ x_2 \end{cases} + \begin{bmatrix} 0 & 0 \\ \frac{1}{m} & 0 \end{bmatrix} \begin{cases} F \\ 0 \end{cases} \quad \text{and} \quad (4a)$$

$$\begin{cases} \dot{x}_1 \\ \dot{x}_2 \end{cases} = \begin{bmatrix} 0 & 1 \\ 0 & -\frac{\alpha}{m}x_1x_2 \end{bmatrix} \begin{cases} x_1 \\ x_2 \end{cases} + \begin{bmatrix} 0 & 0 \\ \frac{1}{m} & 0 \end{bmatrix} \begin{cases} F \\ 0 \end{cases}. \quad (4b)$$

These two SDC representations will be used in Sec. 4 to evaluate weighting matrices.

2.2 Model II

Following the model I description, Eq. 1, a term is added, increasing its nonlinearity and thus complexity

$$m\ddot{x} + \beta x\dot{x} + \alpha x\dot{x}^2 = F. \quad (5)$$

$$\begin{cases} \dot{x}_1 = x_2 \\ \dot{x}_2 = \frac{F}{m} - \frac{\beta}{m}x_1x_2 - \frac{\alpha}{m}x_1x_2^2 \end{cases} \quad (6)$$

Equation 6 allow us to write the systems of equations in matricial form, similarly as for Model I. The extra term from Eq. (5) allows one to write two additional representations, leading to four different SDC A-matrices, such that

$$\begin{cases} \dot{x}_1 \\ \dot{x}_2 \end{cases} = \begin{bmatrix} 0 & 1 \\ -\frac{\beta}{m} & -\frac{\alpha}{m}x_1x_2 \end{bmatrix} \begin{cases} x_1 \\ x_2 \end{cases} + \begin{bmatrix} 0 & 0 \\ \frac{1}{m} & 0 \end{bmatrix} \begin{cases} F \\ 0 \end{cases} \quad (7a)$$

$$\begin{cases} \dot{x}_1 \\ \dot{x}_2 \end{cases} = \begin{bmatrix} 0 & 1 \\ 0 & -\frac{\beta}{m}x_1 - \frac{\alpha}{m}x_1x_2 \end{bmatrix} \begin{cases} x_1 \\ x_2 \end{cases} + \begin{bmatrix} 0 & 0 \\ \frac{1}{m} & 0 \end{bmatrix} \begin{cases} F \\ 0 \end{cases}, \quad (7b)$$

$$\begin{cases} \dot{x}_1 \\ \dot{x}_2 \end{cases} = \begin{bmatrix} 0 & 1 \\ -\frac{\beta}{m}x_2 - \frac{\alpha}{m}x_2^2 & 0 \end{bmatrix} \begin{cases} x_1 \\ x_2 \end{cases} + \begin{bmatrix} 0 & 0 \\ \frac{1}{m} & 0 \end{bmatrix} \begin{cases} F \\ 0 \end{cases} \quad \text{and} \quad (7c)$$

$$\begin{cases} \dot{x}_1 \\ \dot{x}_2 \end{cases} = \begin{bmatrix} 0 & 1 \\ -\frac{\alpha}{m}x_2^2 & -\frac{\beta}{m}x_1 \end{bmatrix} \begin{cases} x_1 \\ x_2 \end{cases} + \begin{bmatrix} 0 & 0 \\ \frac{1}{m} & 0 \end{bmatrix} \begin{cases} F \\ 0 \end{cases}. \quad (7d)$$

It is important to mention that all these SDC refer to the same dynamic model.

armature resistance and motor internal damping, respectively; ρ represents mass per unit length, and γ_1 the assumed first flexural mode constant.

Let the states be given by

$$x_1 = \theta, \quad x_2 = \dot{\theta}, \quad x_3 = q_1 \quad \text{and} \quad x_4 = \dot{q}_1$$

Thus, in the state-space form Eq. (8) is written as

$$\dot{x}_1 = x_2 \tag{9a}$$

$$\dot{x}_2 = pU - ex_2 - fx_4 - gx_3 - kx_2x_3x_4 - wx_3^2x_2 + lx_2^2x_3 \tag{9b}$$

$$\dot{x}_3 = x_4 \tag{9c}$$

$$\dot{x}_4 = qU - rx_2 - sx_4 - tx_3 - vx_2x_3x_4 - zx_3^2x_2 + yx_2^2x_3 \tag{9d}$$

where $e = ac_2 + bc_3$, $f = ac_3 + bc_4$, $g = bc_5$, $k = 2a\gamma_1$, $l = b\rho\gamma_1$, $p = aK_t/R_a$, $q = bK_t/R_a$, $r = bc_2 + dc_3$, $s = bc_3 + dc_4$, $t = dc_5$, $v = 2b\gamma_1$, $w = ac_6$, $z = bc_6$ and $y = d\rho\gamma_1$. Finally leading to a matricial form

$$\begin{pmatrix} \dot{x}_1 \\ \dot{x}_2 \\ \dot{x}_3 \\ \dot{x}_4 \end{pmatrix} = \begin{bmatrix} 0 & 1 & 0 & 0 \\ 0 & -e - wx_3^2 & -g + lx_2^2 & -f - kx_2x_3 \\ 0 & 0 & 0 & 1 \\ 0 & -r - zx_3^2 & -t + yx_2^2 & -s - vx_2x_3 \end{bmatrix} \begin{pmatrix} x_1 \\ x_2 \\ x_3 \\ x_4 \end{pmatrix} + \begin{pmatrix} 0 \\ p \\ 0 \\ q \end{pmatrix} U \tag{10}$$

The last three terms of both Eqs. 9b and 9d indicates the possible SDC factorisations. So, Eq. 10 is one of 144 possible representations.

3 State Dependent Riccati Equation (SDRE) Control

A nonlinear system can be modelled as a state-space system

$$\dot{x} = f(x) + B(x)u.$$

or being $f(x)$ state dependent, such as

$$\dot{x} = A(x)x + B(x)u \tag{11}$$

with feedback control effort described as

$$u = -R^{-1}(x)B^T(x)P(x)x, \tag{12}$$

which is a function of weighting matrix $R(x)$ and $P(x)$. The latter is the solution of the algebraic State Dependent Riccati Equation (SDRE) [2]

$$P(x)A(x) + A^T(x)P(x) + Q(x) - P(x)B(x)R^{-1}(x)B^T(x)P(x) = 0. \tag{13}$$

MATLAB/Octave function LQR calculates the Linear Quadratic Regulator gain $-R^{-1}(x)B^T(x)P(x)$, minimising the performance index

$$J = \frac{1}{2} \int_0^{\infty} [x'(t)Qx(t) + u'(t)Ru(t)] dt. \quad (14)$$

So, from Eq. 14 becomes clear that weighting matrix $Q(x)$ is associated with evolution of states, while $R(x)$ with the control effort. Note that for the general case, both matrices are written as dependent on the current states, and hence may vary with time [3]. SDRE Control requires both matrices to be symmetric, with Q semi-definite positive and R definite-positive, or

$$Q \geq 0$$

$$R > 0$$

Lipschutz and Lipson [8] mention that matrix definite- and positiveness can be verified by calculating its eigenvalues. Being λ_Q and λ_R eigenvalues of Q and R , respectively, thus

$$\lambda_Q \geq 0, \quad \forall \lambda_Q \quad (15)$$

$$\lambda_R > 0, \quad \forall \lambda_R. \quad (16)$$

3.1 Model I & II considerations

Model I and II systems are of the same size, Eqs. 4 and 7, hence require Q and R of same size, i.e., 2×2 . As per matrix positiveness, diagonal terms should be real, equal or greater than zero for Q and real positive for R . Nondiagonal terms might assume any real values, as long as tested according to Eqs. 15 and 16. Gaussian distributions were defined so as to respect the aforementioned range considering position in matrix, centred in zero with high variance, so $\mu = 0$ and $\sigma = 10^{10}$. The sampling method on these distributions resulted in the testing cases.

More information on the resulting matrices will be given in Section 4.

3.2 Model III considerations

The same distributions used for Models I and II were applied to Model III, however Q is 4×4 , while R is 1×1 . Due to large number of required samples to be tested, a slightly small variance was used, $\sigma = 10^9$.

4 Investigation Method

A large set of constant weighting matrices was tested for each model. Among the results of these large sets, the selected samples were sorted with the criteria of respecting a limit time convergence and the amount of energy required to do so. The following items will detail the procedure.

4.1 Random Q and R matrices

UQlab [9] was used to create individual gaussian distributions for each diagonal and nondiagonal of Q and R , always respecting the symmetry conditions. The distributions parameters followed the considerations of Item 3.1 and 3.2, that were afterwards sampled using Monte Carlo method [11]. Important to mention that each generated set formed a matrix that was tested to assure positiveness requirement listed in Eqs. 15 and 16. Figure 2a shows the full set of samples for first diagonal term for matrix Q , respecting the positive real restriction. The "selected" refers to the terms that belong to matrices that respect the

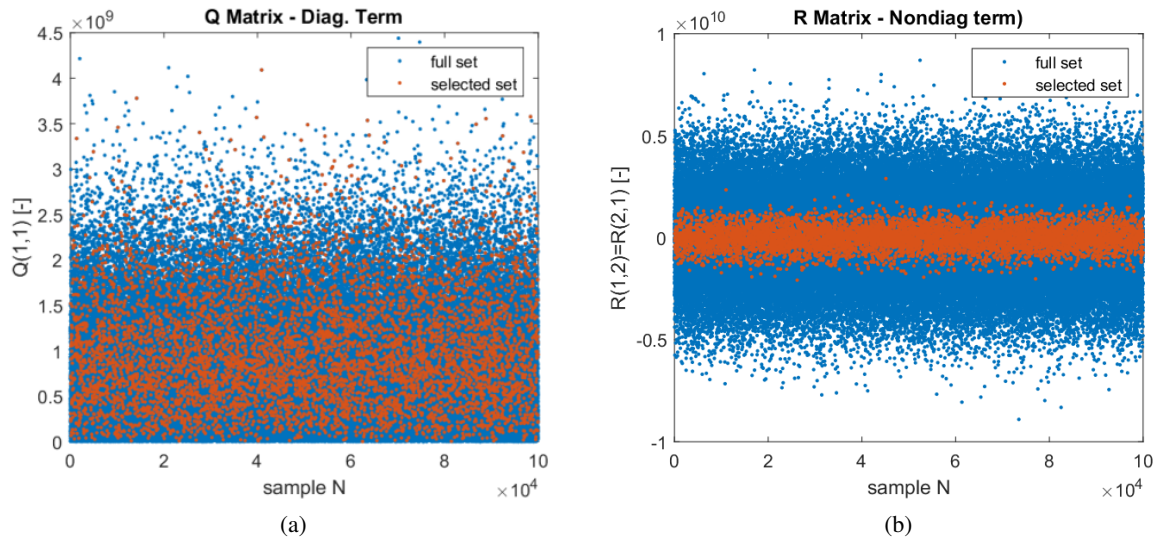


Figure 2. Samples terms of matrices Q and R . The number of selected samples was 6605 out of the generated 10^5 .

requirements. Accordingly, Fig. 2b show a nondiagonal term from R . Note that these values now can assume any real value. The same procedure was made to obtain Q and R for model III.

4.2 Initial Conditions and Model Parameters

The equations from Model I – Eqs. 4, Model II – Eqs. 7 and Model III – Eq. 10, were implemented in MATLAB and integrated using Runge-Kutta 4th order with fixed timestep [10]. The calculation of gain from Eq. 12 was performed at the beginning of each step of integration, with control effort $u(x)$, $A(x)$ and $B(x)$ recalculated intrastep.

The parameters and initial conditions to simulate Model I, II and III are presented in Tabs. 1-2. Model III remaining parameters are shown in Tab. 3.

Table 1. Parameters and initial conditions for models I and II.

Variable		Unit
x_1	10	[m]
x_2	0	[m/s]
m	2	[kg]
α	500	[-]
β	100	[-]
Δt	0.01	[s]
t_0	0	[s]
t_f	20	[s]

Table 2. Parameters and initial conditions for model III.

State	Case 1	Case2	Unit
x_1	0.1745	0.8727	[rad]
x_2	0	0	[rad/s]
x_3	0	0	[m]
x_4	0	0	[m/s]
Δt	0.001	0.001	[s]
t_0	0	0	[s]
t_f	10	10	[s]

Table 3. Model III parameters.

Parameters		Unit
L	2	[m]
E	70	[GPa]
I	5.6250E-12	[m ⁴]
I	5.6250E-12	[m ⁴]
C_D	1.1	[-]
K_t	0.0528140	[Vs/rad]
K_b	0.0528140	[Nm/A]
I_{motor}	0.0000654	[kg/m ²]
R_a	1.9149520	[Ω]
R_a	0.0031000	[H]
C_m	0.0046290	[Nms/rad]
ρ	2700	[kg/m ³]

5 Results

The models SDCs were simulated with selected constant Q and R matrices using the aforementioned parameters and initial conditions. The results were separated into the following items.

5.1 Model I

Figures 3a-3f show the results for x_1 , \dot{x}_1 and u for model I SDC representations, Eq. 4. Both SDC give a variety of results with the wide range of Q and R used. Note that several sets results could not reach zero, meaning that they could not converge with the available time, Fig. 3a and 3d. In addition, SDC 1 gives a greater negative overshoot than SDC 2. For that reason, Fig. 3b shows positive values for \dot{x}_1 , that almost cannot be seen in SDC 2, Fig. 3e. For both SDCs, u almost ceases with $t = 5s$.

The absolute value of control effort u for all sets that reach $x_1 = 0$ was integrated over time to establish an energy analogous. These results were then sorted, with the first four of each SDC plotted in Figs. 4a-4d. Although the aggregated results showed different tendencies, when the least energy sets are compared in Fig. 4d, they appear more similar. Also, SDC 2 provides the four chosen sets closer to each other than the SDC 1. So, one can affirm that for this specific model and these initial conditions, both SDCs shows similar suboptimal results.

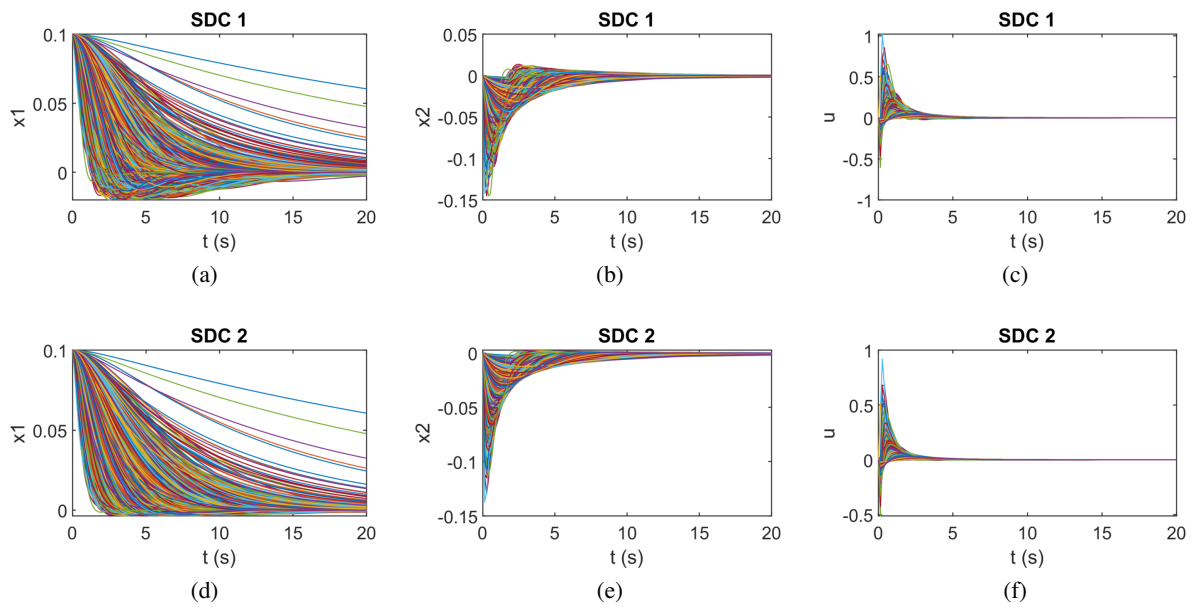


Figure 3. Model I results for all simulated sets of random matrices.

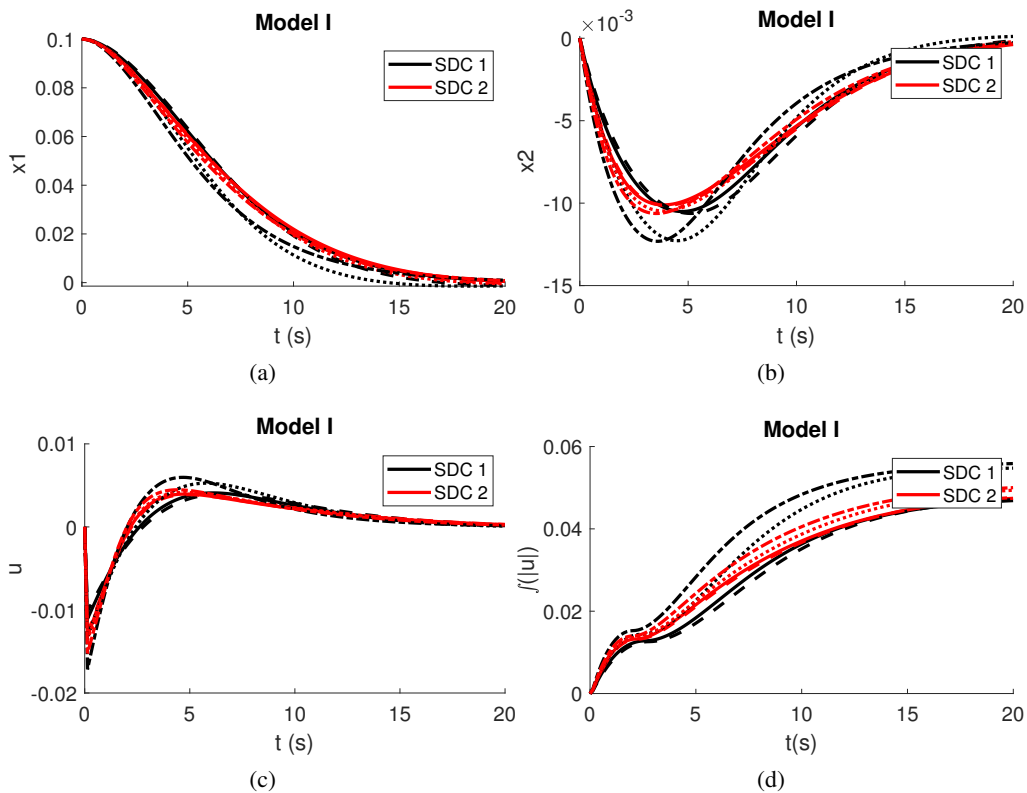


Figure 4. Model I - Least 'energy' curves sorted as ascending order '...', '-...', '...', and '...',..

The 'least-energy' analysis sorted the following weighting matrices samples for SDC-1

$$\begin{array}{l}
 S : 1438 \quad Q = 10^8 \begin{bmatrix} 0.07631 & -0.35714 \\ & 1.93203 \end{bmatrix} \quad R = 10^8 \begin{bmatrix} 6.44231 & -1.77308 \\ & 3.43462 \end{bmatrix} \\
 S : 4330 \quad Q = 10^8 \begin{bmatrix} 0.11847 & +0.19286 \\ & 2.49537 \end{bmatrix} \quad R = 10^9 \begin{bmatrix} 1.19926 & -0.50927 \\ & 1.57918 \end{bmatrix} \\
 S : 2360 \quad Q = 10^8 \begin{bmatrix} 0.20161 & +0.23611 \\ & 3.10594 \end{bmatrix} \quad R = 10^9 \begin{bmatrix} 1.25412 & -0.54302 \\ & 1.24291 \end{bmatrix} \\
 S : 1813 \quad Q = 10^9 \begin{bmatrix} 0.08930 & +0.33317 \\ & 1.94823 \end{bmatrix} \quad R = 10^9 \begin{bmatrix} 2.72680 & -0.61663 \\ & 2.41415 \end{bmatrix}
 \end{array} \tag{17}$$

and SDC-2

$$\begin{array}{l}
 S : 2360 \quad Q = 10^8 \begin{bmatrix} 0.20161 & +0.23611 \\ & 3.10594 \end{bmatrix} \quad R = 10^9 \begin{bmatrix} 1.25412 & -0.54302 \\ & 1.24291 \end{bmatrix} \\
 S : 629 \quad Q = 10^8 \begin{bmatrix} 0.40901 & -0.53590 \\ & 5.01121 \end{bmatrix} \quad R = 10^9 \begin{bmatrix} 2.46574 & +0.46331 \\ & 0.93964 \end{bmatrix} \\
 S : 2735 \quad Q = 10^8 \begin{bmatrix} 0.32556 & +0.70160 \\ & 3.68050 \end{bmatrix} \quad R = 10^9 \begin{bmatrix} 1.65939 & +0.34374 \\ & 1.23680 \end{bmatrix} \\
 S : 5174 \quad Q = 10^8 \begin{bmatrix} 0.28745 & -0.11438 \\ & 4.86463 \end{bmatrix} \quad R = 10^9 \begin{bmatrix} 1.63950 & -0.96704 \\ & 1.65291 \end{bmatrix}
 \end{array} \tag{18}$$

Equations 17-18 present the 'least-energy' weighting matrices Q and R for both SDCs. Since the matrices are symmetric, the lower nondiagonal terms were omitted. Note that the order of magnitude for all Q and R are similar. The difficulty of choosing SDC representation and Q and R can be exemplified by observing that Sample $S : 2360$ – least-energy for SDC-2 – is only the third for SDC-1. In addition, weighting matrices look quite different, even if similar results are obtained for the same or different SDC.

5.2 Model II

The same procedure of Item 5.1 was used to infer Model II SDCs behaviour, resulting in Figs. 5a-5l. The first plots row shows that SDCs 1 and 3 are similar and less sensitive to Q and R , allowing almost all sets to converge before $t = 20$ s. On the other hand, SDCs 2 and 4 allow to infer a broader performance envelope. The velocities, \dot{x}_2 , also corroborates to the idea of swiping a broader envelope. Control effort u , Figs. 5i-5l, indicates that SDCs 1 and 3 faster convergence occurs due to higher u values.

Integrating absolute u over time, sorting the results and choosing four converged sets per SDC, one obtains Figs. 6a-6d. Differently from Model I, the SDCs gave constrasting results. SDCs 2 and 4 x_1 state reach zero with a smaller velocity, Fig. 6b, result from different integrated u curve shape, Fig.6d. As discussed before, SDCs 1 and 3 gave more consistent results, probably for being less sensitive to the chosen Q and R .

Sample matrices that resulted in least-energy for SDC-1 and 3 were equal, the same for SDC-2 and 4. For that reason, they are grouped in Eqs. 19-20. Differently from Model I, $S : 5922$ sampled matrices resulted in least-energy for all SDCs. However, although the $\int(|u|)$ have almost equal values at $t = 20$ s,

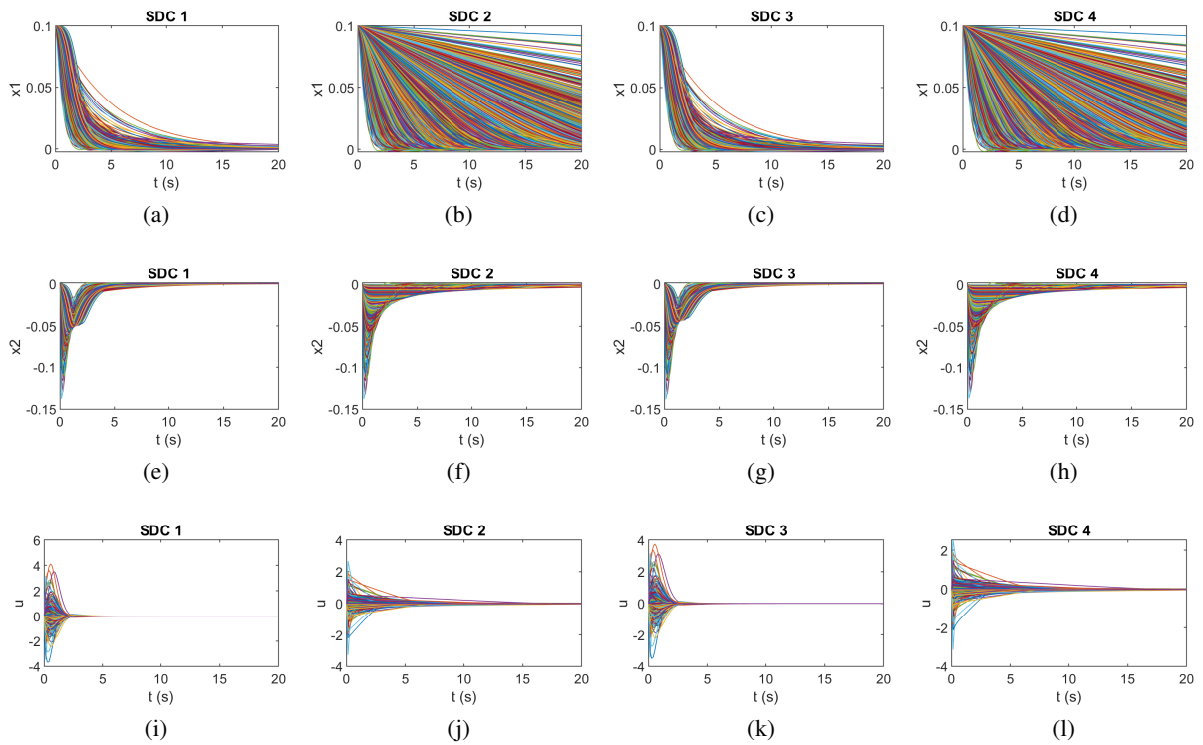


Figure 5. Model II results for all simulated sets of random matrices.

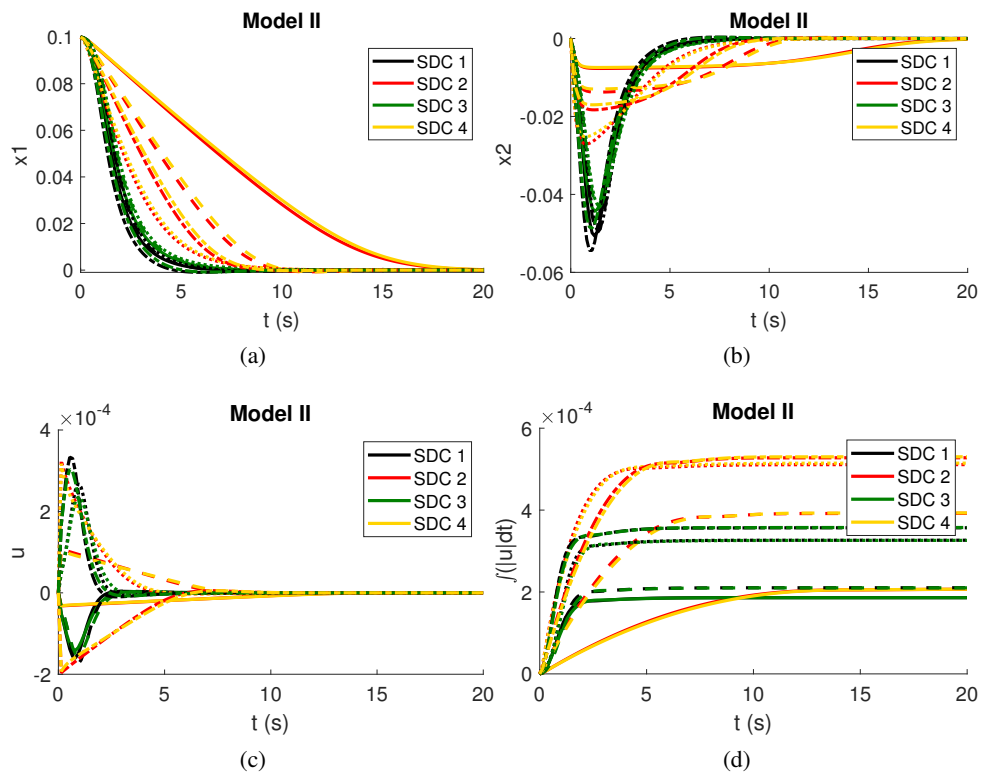


Figure 6. Model II - Least 'energy' curves sorted as ascending order '-,-,-,-' and '-.-'.

the evolution is completely different, as can be seen in Fig.6. Concerning samples that appear in both groups, $S : 5145$ is fourth at SDC1-3, while second in SDC2-4, giving different evolution, but similar final results.

Sampled weighting matrices for SDC 1-3

$$\begin{array}{l}
 S : 5922 \quad Q = 10^8 \begin{bmatrix} 2.92965 & +3.65104 \\ & 9.48856 \end{bmatrix} \quad R = 10^8 \begin{bmatrix} 5.02544 & -0.00362 \\ & 8.50107 \end{bmatrix} \\
 S : 5144 \quad Q = 10^9 \begin{bmatrix} 0.25495 & -0.17407 \\ & 1.54859 \end{bmatrix} \quad R = 10^9 \begin{bmatrix} 1.28086 & -0.00097 \\ & 2.05178 \end{bmatrix} \\
 S : 4699 \quad Q = 10^9 \begin{bmatrix} 0.13544 & +0.37925 \\ & 1.35824 \end{bmatrix} \quad R = 10^8 \begin{bmatrix} 8.41588 & +0.00429 \\ & 5.80279 \end{bmatrix} \\
 S : 5145 \quad Q = 10^9 \begin{bmatrix} 1.26769 & +0.38996 \\ & 0.18398 \end{bmatrix} \quad R = 10^9 \begin{bmatrix} 0.70557 & +0.00129 \\ & 1.58628 \end{bmatrix}
 \end{array} \tag{19}$$

and SDC 2-4

$$\begin{array}{l}
 S : 5922 \quad Q = 10^8 \begin{bmatrix} 2.92965 & +3.65104 \\ & 9.48856 \end{bmatrix} \quad R = 10^8 \begin{bmatrix} 5.02544 & -0.00036 \\ & 8.50107 \end{bmatrix} \\
 S : 5145 \quad Q = 10^9 \begin{bmatrix} 1.26769 & +0.38996 \\ & 0.18398 \end{bmatrix} \quad R = 10^9 \begin{bmatrix} 0.70557 & +0.00129 \\ & 1.58628 \end{bmatrix} \\
 S : 623 \quad Q = 10^9 \begin{bmatrix} 0.37289 & -0.03658 \\ & 1.03759 \end{bmatrix} \quad R = 10^8 \begin{bmatrix} 0.38708 & +0.00589 \\ & 5.07238 \end{bmatrix} \\
 S : 1322 \quad Q = 10^9 \begin{bmatrix} 2.10502 & -1.41791 \\ & 1.68649 \end{bmatrix} \quad R = 10^9 \begin{bmatrix} 0.64627 & -0.00233 \\ & 2.08590 \end{bmatrix} .
 \end{array} \tag{20}$$

5.3 Model III

Model III equations were evaluated for a set of 5687 Q and R sets and integrated for load case I and II, resulting in the plots in Figs. 7a-7j. The general aspect of x_1 for both load cases, Figs. 7a and 7f, resembles a combination of Model II SDCs 1-3 and SDCs 2-4, Figs. 5a-5d. The more disperse the results are, the easier one might extract possible scenarios. However, a few of the sets did not provide means to reach zero, not stabilising the system during the simulated time.

Comparing the results for load cases 1 and 2, Figs. 7a-7e and Figs. 7f-7j, one notes that curve shapes are similar, being scaled by a large factor for load case 2. Hence, the higher the initial conditions x_1 , the greater the velocities and control effort.

Absolute control effort results were integrated over time, sorted in ascending order. The first five were selected, grouped, and plotted for load cases 1 and 2, Figs. 8a and 8l, respectively. It is possible to observe that a few sets of Q and R converge faster than the least energy cases, but probably with a higher u , peak velocity and thus penalising the required energy.

The selected least energy weighting matrices are shown in Eq. 21. It is possible to observe that for the five least-energy cases the order of magnitude for both Q and R are the same. Not all nondiagonal terms are always positive or negative, indicating that nonzero values can indeed produce interesting results. In addition, results shown in Fig. 8 imply the close equivalence of these five least-energy sample

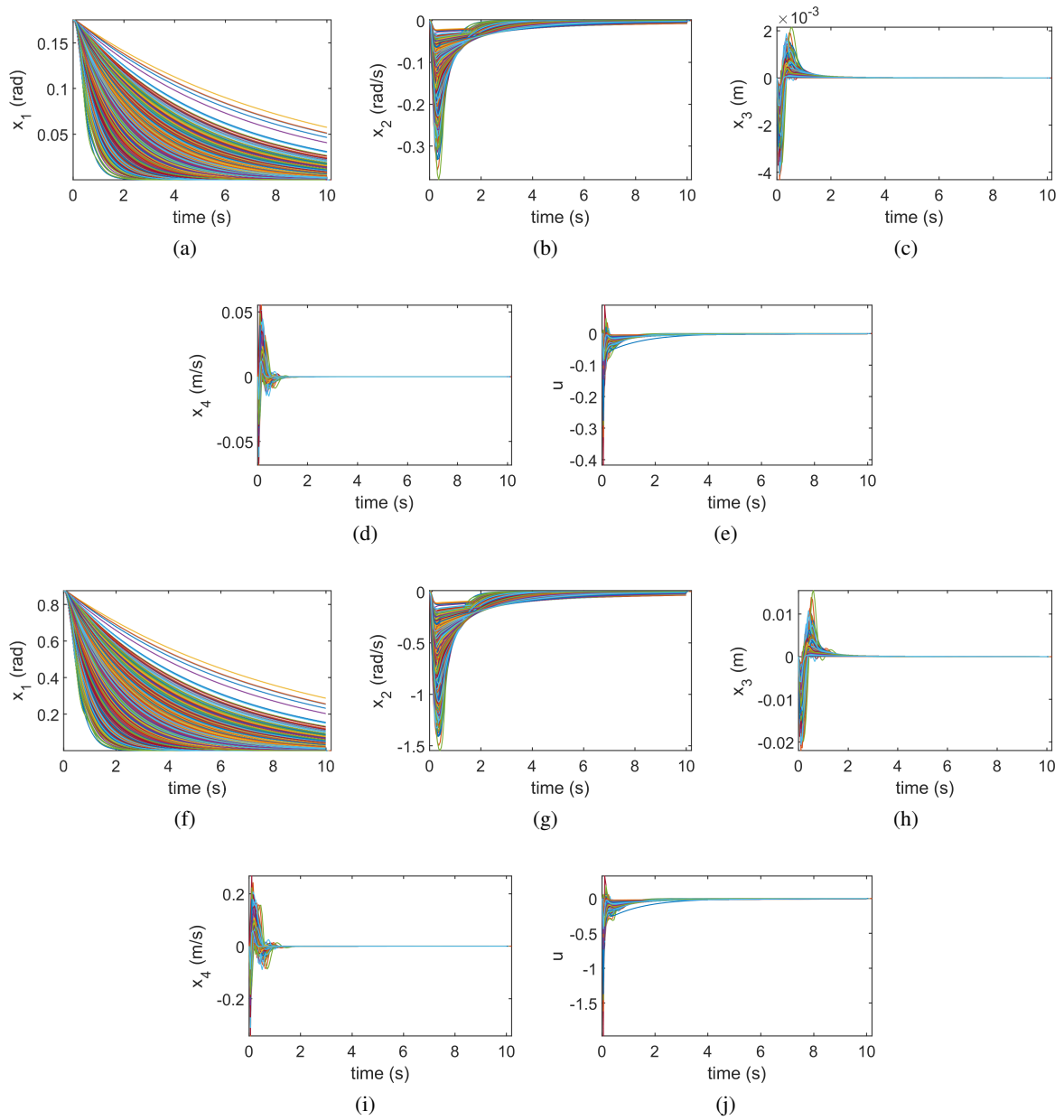


Figure 7. Model III results for load case I and II

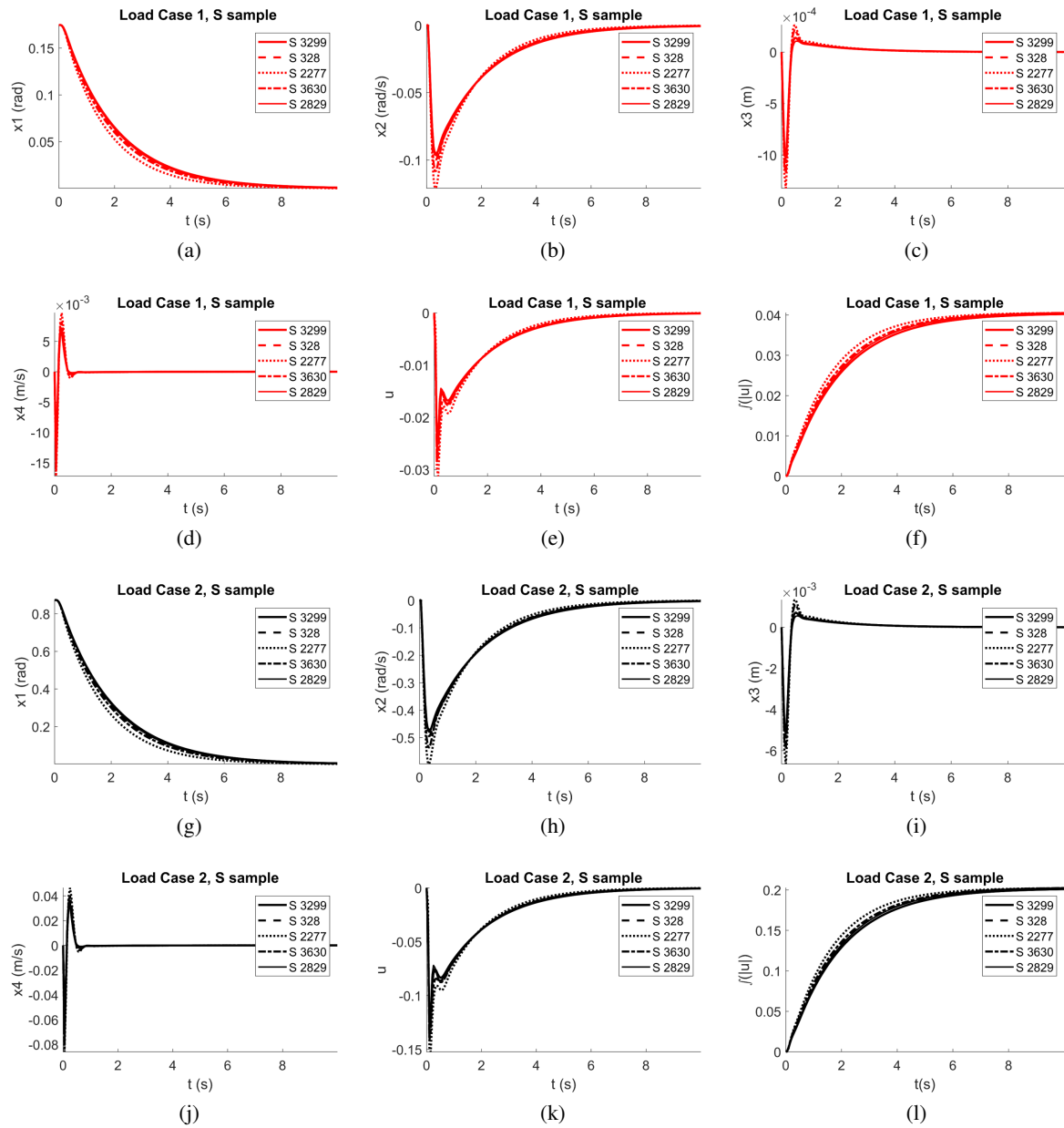


Figure 8. Model III - Least 'energy' curves sorted as ascending order '-','-',':','-' and '-'.

matrices and that can be a sign that the Q and R terms are almost equivalent. If one multiplies Q and R for the same scalar, the optimisation procedure would result in the same performance index, Eq. 14, hence the same states and control effort.

$$\begin{aligned}
 S : 3299 \quad Q = 10^9 & \begin{bmatrix} 0.14851 & +0.18371 & -0.16622 & -0.09322 \\ & 0.36773 & -0.32453 & -0.09579 \\ & & 1.43156 & -0.79603 \\ & & & 1.30961 \end{bmatrix} R = 10^8 [6.31849] \\
 S : 328 \quad Q = 10^9 & \begin{bmatrix} 0.26130 & +0.23897 & +0.14820 & +0.21039 \\ & 0.59817 & +0.67624 & -0.23474 \\ & & 2.27110 & +0.07465 \\ & & & 2.06779 \end{bmatrix} R = 10^8 [8.79359] \\
 S : 2277 \quad Q = 10^9 & \begin{bmatrix} 0.22223 & +0.08361 & +0.13119 & -0.01131 \\ & 0.36139 & +0.53200 & +0.17547 \\ & & 1.170605 & +0.69554 \\ & & & 1.03593 \end{bmatrix} R = 10^8 [8.30370] \quad (21) \\
 S : 3630 \quad Q = 10^9 & \begin{bmatrix} 0.16679 & +0.10273 & +0.36592 & +0.08082 \\ & 0.36043 & +0.25777 & +0.23788 \\ & & 0.82016 & +0.35273 \\ & & & 2.25461 \end{bmatrix} R = 10^8 [5.39829] \\
 S : 2829 \quad Q = 10^9 & \begin{bmatrix} 0.28394 & -0.22676 & -0.28041 & +0.64627 \\ & 0.68383 & +0.24652 & -0.77017 \\ & & 1.25420 & -0.69405 \\ & & & 1.76055 \end{bmatrix} R = 10^8 [8.17706].
 \end{aligned}$$

6 Concluding Remarks

A method to evaluate the performance of SDRE controlled system was here presented. Three non-linear models were evaluated by using a large set of constant weighting matrices (Q and R) obtained by Monte Carlo sampling of gaussian distributions. Weighting matrices need not to be constant and setting state dependent Q and R might lead to interesting performance results [1–3]. However, the designer might need experience to penalise a specific term of a Q and/or R , that can also be troublesome. Thus, the presented method allows one to investigate a system performance envelope using simple constant weighting matrices, without the need of prior system knowledge.

Weighting matrices can be varied during simulation for evaluation purposes. However, the amount of computational cost and generated data might be prohibitive. Criteria based on maximum/minimum states or u may lead to results that are within the system and/or actuator limits. However, establishing an integrated criteria during simulation may trap the solution in a local minimum. For instance, Fig. 6d shows that 'energy' for SDCs 2 and 4 were smaller than SDC 1 and 3 until $t = 10$ s, becoming greater

after that instant. Hence, defining a criteria to choose only one set for a specific instant may result in a not so optimal global solution. To tackle this problem, one might record all data for simulations varying Q and R each step, but that may be impractical for costly simulations.

Multiplying Q and R by a single scalar may result in exactly the same performance index, Eq. 14, and thus the same x and u . So, in a future work, it is expected that generated sample matrices form independent basis, which cannot be obtained by simply multiplying another sample by a single scalar, thus enriching the analysis.

The complexity of investigating performance envelope might be reduced if the simulated SDCs are a composition of two distinct SDC as suggested by Cloutier et al. [3], but also if the designer establish a range of possible Q and R terms and sample their distributions without concerning physical meaning. Moreover, physical system limitations as maximum gain, energy or force, can be verified to choose candidate sets.

Acknowledgements

The authors would like to thank Victoria de S. Rodrigues and Roney Duarte da Silva for the valuable discussions.

References

- [1] Naidu, D. S., 2002. *Optimal Control Systems*. Electrical Engineering Series. CRC Press, 1 edition.
- [2] Çimen, T., 2008. State-dependent riccati equation (sdre) control: A survey. *IFAC Proceedings Volumes*, vol. 41, n. 2, pp. 3761 – 3775. 17th IFAC World Congress.
- [3] Cloutier, J., D’Souza, C., & Mracek, C., 1994. Nonlinear regulation and nonlinear H_∞ control via the state-dependent riccati equation technique: Part 1, theory. vol. .
- [4] Nahshon, K., Reynolds, N., & Shields, M. D., 2018. Efficient uncertainty propagation for high-fidelity simulations with large parameter spaces: Application to stiffened plate buckling. *ASME. J. Verif. Valid. Uncert.*, vol. , n. 1, pp. 16.
- [5] Nguyen, H. X., Hien, T. D., Lee, J., & Nguyen-Xuan, H., 2017. Stochastic buckling behaviour of laminated composite structures with uncertain material properties. *Aerospace Science and Technology*, vol. 66, pp. 274 – 283.
- [6] Pellissetti, M. & Schuëller, G., 2009. Scalable uncertainty and reliability analysis by integration of advanced monte carlo simulation and generic finite element solvers. *Computers & Structures*, vol. 87, n. 13, pp. 930 – 947.
- [7] Fenili, A. & Francisco, C. P. F., 2010. Position and vibration control of a nonlinear slewing flexible structure considering fluid-structure interaction. In *ICNPAA 2010 World Congress*.
- [8] Lipschutz, S. & Lipson, M., 2017. *Schaum’s Outline of Linear Algebra, Sixth Edition*. McGraw-Hill Education.
- [9] Marelli, S. & Sudret, B., 2014. *UQLab: A Framework for Uncertainty Quantification in Matlab*, pp. 2554–2563.
- [10] Chapra, S. & Canale, R., 2009. *Numerical Methods for Engineers*. McGraw-Hill Education.
- [11] Helton, J. & Davis, F., 2003. Latin hypercube sampling and the propagation of uncertainty in analyses of complex systems. *Reliability Engineering & System Safety*, vol. 81, n. 1, pp. 23 – 69.